


## RESEARCH ARTICLE

## The plasma miRNAome in ADNI: Signatures to aid the detection of at-risk individuals

Dennis M. Krüger<sup>1,2</sup> | Tonatiuh Pena-Centeno<sup>1,2</sup> | Shiwei Liu<sup>3</sup> | Tamina Park<sup>3</sup> |  
 Lalit Kaurani<sup>1</sup> | Ranjit Pradhan<sup>1</sup> | Yen-Ning Huang<sup>3</sup> | Shannon L. Risacher<sup>3</sup> |  
 Susanne Burkhardt<sup>1</sup> | Anna-Lena Schütz<sup>4</sup> | Yang Wan<sup>5</sup> | Leslie M. Shaw<sup>5</sup> |  
 Alexander S. Brodsky<sup>6</sup> | Anita L. DeStefano<sup>7</sup> | Honghuang Lin<sup>8</sup> | Robert Schroeder<sup>1</sup> |  
 Andre Kronic<sup>9</sup> | Nina Hempel<sup>1</sup> | Farahnaz Sananbenesi<sup>4</sup> | Jan Krzysztof Blusztajn<sup>9</sup> |  
 Andrew J. Saykin<sup>10</sup> | Ivana Delalle<sup>9</sup>  | Kwangsik Nho<sup>10</sup> | Andre Fischer<sup>1,11,12,13</sup> |  
 Alzheimer's Disease Neuroimaging Initiative

<sup>1</sup>Department for Epigenetics and Systems Medicine in Neurodegenerative Diseases, German Center for Neurodegenerative Diseases (DZNE), Göttingen, Germany

<sup>2</sup>Bioinformatics Unit, German Center for Neurodegenerative Diseases (DZNE), Göttingen, Germany

<sup>3</sup>Center for Computational Biology and Bioinformatics, Indiana University School of Medicine, Indianapolis, Indiana, USA

<sup>4</sup>Research Group for Genome Dynamics in Brain Diseases, German Center for Neurodegenerative Diseases, Göttingen, Germany

<sup>5</sup>Perelman School of Medicine, Department of Pathology and Laboratory Medicine, University of Pennsylvania, Philadelphia, Pennsylvania, USA

<sup>6</sup>Department of Pathology and Laboratory Medicine, Rhode Island Hospital, Warren Alpert Medical School at Brown University, Providence, Rhode Island, USA

<sup>7</sup>Department of Biostatistics, Boston University School of Public Health, Boston, Massachusetts, USA

<sup>8</sup>Department of Medicine, UMass Chan Medical School, Worcester, Massachusetts, USA

<sup>9</sup>Department of Pathology & Laboratory Medicine, Boston University Chobanian & Avedisian School of Medicine, Boston, Massachusetts, USA

<sup>10</sup>Department of Radiology and Imaging Sciences and the Indiana Alzheimer's Disease Research Center, Indiana University School of Medicine, Indianapolis, Indiana, USA

<sup>11</sup>Department for Psychiatry and Psychotherapy, University Medical Center of Göttingen, Georg-August University, Göttingen, Germany

<sup>12</sup>Cluster of Excellence "Multiscale Bioimaging: from Molecular Machines to Networks of Excitable Cells" (MBExC), University of Göttingen, Göttingen, Germany

<sup>13</sup>German Center for Cardiovascular Diseases (DZKH) Göttingen, Göttingen, Germany

## Correspondence

Ivana Delalle, Department of Pathology & Laboratory Medicine, Boston University Chobanian & Avedisian School of Medicine, 670 Albany St, Boston, MA 02118, USA.  
 Email: [idelalle@bu.edu](mailto:idelalle@bu.edu)

Andrew J. Saykin, Ivana Delalle, Kwangsik Nho, and Andre Fischer directed the study.

## Funding information

NIH, Grant/Award Numbers: RF1AG078299, AG067188, P30AG010133, P30AG072976,

## Abstract

**INTRODUCTION:** MicroRNAs are short non-coding RNAs that control proteostasis at the systems level and are emerging as potential prognostic and diagnostic biomarkers for Alzheimer's disease (AD).

**METHODS:** We performed small RNA sequencing on plasma samples from 847 Alzheimer's Disease Neuroimaging Initiative (ADNI) participants.

**RESULTS:** We identified microRNA signatures that correlate with AD diagnoses and help predict the conversion from mild cognitive impairment (MCI) to AD.

Dennis M. Krüger, Tonatiuh Pena-Centeno, Shiwei Liu, and Tamina Park contributed equally to this study.

This is an open access article under the terms of the [Creative Commons Attribution-NonCommercial-NoDerivs](https://creativecommons.org/licenses/by-nc-nd/4.0/) License, which permits use and distribution in any medium, provided the original work is properly cited, the use is non-commercial and no modifications or adaptations are made.

© 2024 The Author(s). *Alzheimer's & Dementia* published by Wiley Periodicals LLC on behalf of Alzheimer's Association.

ADNI4, P30PENNADRC, U01AG068221-01A1, R01AG080670, P30AG073107, RF1AG057768, P30AG013846, RF1AG072654, U01AG058589, R01DK122503, P30AG072978, U19AG068753, R01AG019771, R01AG057739, U19AG024904, R01LM013463, R01AG068193, T32AG071444, U01AG068057, U01AG072177, U19AG074879; DFG (Deutsche Forschungsgemeinschaft) Priority Program, Grant/Award Numbers: 1738, SFB1286, GRK2824; German Federal Ministry of Science and Education, Grant/Award Number: EPINEURODEVO; EU Joint Programme-Neurodegenerative Diseases (JPND), Grant/Award Number: EPI-3E; Germany's Excellence Strategy, Grant/Award Number: EXC 2067/1 390729940; GoBio Project miRassay, Grant/Award Number: 16LW0055; Alzheimer's Association, Grant/Award Number: AARG-NTF-20-643020; American Heart Association, Grant/Award Number: 20SFRN35460034

**DISCUSSION:** Our data demonstrate that plasma microRNA signatures can be used to not only diagnose MCI, but also, critically, predict the conversion from MCI to AD. Moreover, combined with neuropsychological testing, plasma microRNAome evaluation helps predict MCI to AD conversion. These findings are of considerable public interest because they provide a path toward reducing indiscriminate utilization of costly and invasive testing by defining the at-risk segment of the aging population.

#### KEYWORDS

Alzheimer's disease, blood biomarker, cognitive decline, microRNA, mild cognitive impairment, plasma, small non-coding RNA

#### Highlights

- We provide the first analysis of the plasma microRNAome for the ADNI study.
- The levels of several microRNAs can be used as biomarkers for the prediction of conversion from MCI to AD.
- Adding the evaluation of plasma microRNA levels to neuropsychological testing in a clinical setting increases the accuracy of MCI to AD conversion prediction.

## 1 | BACKGROUND

The need to improve diagnostic tools for the early detection of Alzheimer's disease (AD)-related neuropathologic processes is paramount for developing prevention and treatment strategies. Because the deterioration of cognitive functions in AD develops slowly over time, patients are currently diagnosed at an advanced stage of neuropathologic changes.<sup>1</sup> Indeed, the failure to diagnose AD at an early stage of molecular pathology is considered the major reason why multiple treatments have failed in clinical trials.<sup>2</sup> Cerebrospinal fluid (CSF) Aβ42, total-TAU (tTAU), and pTAU181 (tau phosphorylated at threonine 181)<sup>3</sup> are considered core biomarkers to support AD diagnosis; however, the invasive nature of obtaining CSF samples limits broad use.<sup>4,5</sup> To address this, several advancements in utilizing blood amyloid-beta and tau as disease biomarkers have been made.<sup>6-9</sup> Nevertheless, the urgent need for novel biomarkers of early AD pathogenesis persists.

MicroRNAs (miRNAs, miRs) are 19–22 nucleotide long RNA molecules that govern protein homeostasis via binding to a target mRNA thereby causing its degradation or inhibition of translation.<sup>10</sup> Circulating miRNAs have been suggested as potential AD biomarkers for several reasons. First, because one miRNA can affect many mRNA targets that are often functionally linked, changes in the levels of a few miRNAs can reflect alterations of multiple key pathways involved in cellular homeostasis.<sup>11,12</sup> Interestingly, microRNAs can also act in a paracrine manner and participate in inter-organ communication,<sup>13-16</sup> indicating that the analysis of circulating microRNAs can inform about pathological alterations in the brain.<sup>17,18</sup> Second,

miRNAs are extremely stable in cell-free environments and resistant to thaw-freeze cycles, making them logistically desirable in a clinical setting.<sup>19,20</sup> Third, blood miRNAome analysis is minimally invasive and inexpensive, making such analysis a potentially ideal first step toward identifying individuals in need of further diagnostic procedures.

Because of their documented role in synaptic plasticity and memory function, miRNAs have been intensively studied in the context of AD.<sup>21,22</sup> However, the interpretation of the reports on changes in miRNA expression in the biospecimens of AD patients are often hampered by small sample size and/or incomplete information on relevant phenotypes which together have prevented the consideration of microRNAs as a biomarker detecting individuals at risk for developing AD.<sup>23</sup> To that end, the Alzheimer's Disease Neuroimaging Initiative (ADNI) represents an unparalleled resource for providing the optimal panel of clinical assessments, magnetic resonance imaging (MRI) and positron emission tomography (PET) imaging measures, and biomarkers in blood and CSF. Cognitive phenotypes obtained in ADNI have been successfully used to enhance clinical trial design, taking advantage of available CSF and plasma samples to study candidate biomarkers.<sup>24-26</sup> The first phase (ADNI1) launched a cohort study composed AD patients, individuals with mild cognitive impairment (MCI), and cognitively normal older adults (controls, CN). Three more phases followed, ADNI-GO, which introduced the concept of early MCI (EMCI), ADNI2, and now the ongoing ADNI3 studies. Here we present the results of the analysis of the first ADNI plasma microRNAome performed on cross-sectional samples from 847 participants in ADNI1/GO/2. Our data demonstrate that plasma microRNA signatures can not only diagnose AD but also help predict the conversion from MCI to AD. Moreover, our data suggest that a blood draw for microRNAome evaluation, combined with neuropsychological testing,

## RESEARCH IN CONTEXT

- 1. Systematic review:** We conducted a PubMed search on circulating microRNAs associated with mild cognitive impairment (MCI), dementia, and Alzheimer's disease (AD). Several plasma, serum, or exosomal microRNAs have been described previously in association with these conditions, and proposed as their biomarkers. However, there is insufficient information on the predictive value of the circulating microRNA levels and the progression of cognitive decline.
- 2. Interpretation:** Our findings, obtained by analyzing the Alzheimer's Disease Neuroimaging Initiative (ADNI) cohort, provide evidence that the levels of specific plasma microRNAs are associated with specific disease states, including early and late stages of MCI and AD. In addition, the levels of several microRNAs can be used as biomarkers for the prediction of conversion from normal cognition to MCI to AD.
- 3. Future directions:** The circulatory microRNA biomarkers identified here will need further validation and refinement in association with clinical, neuropathological, and other molecular markers of MCI and AD.

could become a suitable tool to predict MCI to AD conversion, thus reducing the need for more invasive CSF studies of A $\beta$ 42, total-tau, and P-tau181 levels during initial diagnostic work-up. These findings are of considerable public interest because they provide a path toward reducing the indiscriminate use of costly and invasive testing.

## 2 | METHODS

### 2.1 | Participants

We originally selected cross-sectional plasma samples from 847 ADNI participants; however, the samples from 44 subjects did not meet small RNAseq quality standards as described in Section 3.1. The 803 samples analyzed in this study were obtained from ADNI1/GO/2 participants categorized as CN = 165, EMCI = 272, late MCI (LMCI) = 217, and AD = 149 (Tables S1 and S2).

### 2.2 | Small RNA isolation

A total of 862 plasma samples underwent small RNA isolation followed by small RNA sequencing. Among these, 847 samples were from probands diagnosed with AD or MCI (early/late), or from controls (CN). The remaining 15 samples were randomly selected duplicates. Samples arrived in four shipments and were stored at  $-80^{\circ}\text{C}$ . Upon

arrival, samples were checked to confirm tube labeling and cryobox location. To mitigate batch effects, the 862 samples were distributed across 21 batches based on shipment, gender, and diagnosis. This allocation was done blindly to the phenotype with assistance from ADNI Biomarker core co-Director, Dr. Lesley Shaw, and his team. Small RNA isolation was carried out in 21 batches using the Norgen Biotek Corp. Plasma/Serum RNA Purification Kit (Cat. No. 55000) following the user manual. Initially, two aliquots of 200  $\mu\text{L}$  plasma/individual were thawed at room temperature for 15 min. Some plasma samples showed a white precipitate, which was documented. The tubes were then centrifuged ( $3000 \times g$  at  $4^{\circ}\text{C}$ ), and the supernatant was transferred into a 2 mL Eppendorf tube to which 600  $\mu\text{L}$  of lysis buffer A was added. After vortexing for 10 s, 800  $\mu\text{L}$  of 99.6% ethanol (Roth) was added and vortexed for another 10 s. The mixture was then pipetted onto the micro spin column and centrifuged for 2 min at  $3300 \times g$ . Since the column could only accept 650  $\mu\text{L}$ , this step was repeated until all supernatant were added. The flow-through was discarded, and the columns were washed three times by adding 400  $\mu\text{L}$  wash solution A followed by 30 s of centrifugation at  $3330 \times g$ . Again, the flow-through was discarded, and the columns were centrifuged for 2 min at  $13000 \times g$ . All steps were performed at  $4^{\circ}\text{C}$ . The spin column was added to a new elution collection tube, and 22  $\mu\text{L}$  Elution buffer was added and incubated at room temperature for 2 min. Samples were then centrifuged for 1 min at  $400 \times g$  followed by 2 min at  $5800 \times g$ . The flow-through was again added to the spin column and subjected to the above-described procedure. Finally, the yields from two aliquots of plasma originating from the same proband were pooled to obtain approximately 35  $\mu\text{L}$  of isolated small RNA. 1  $\mu\text{L}$  of small RNA elution was subjected to quality control (QC) using Qubit (Thermo Fisher) to document the concentration. Another 1  $\mu\text{L}$  was used to test RNA quality via a Bioanalyzer (Agilent) using the RNA Pico Assay.

### 2.3 | Small RNA sequencing

Small RNA sequencing was performed for the 21 batches using the QIAseq miRNA NGS 96 Index IL (Qiagen, cat# 331565) for indexes along with the QIAseq miRNA Library Kit (Qiagen, cat# 331505). In each batch, we prepared 41 ADNI samples and 7 samples from a pool of control plasma prepared according to ADNI standard operating procedure (SOP). These 7 samples (batch control samples) served as internal controls and were processed along with each of the 21 batches. Library preparation followed the user manual. Briefly, 5  $\mu\text{L}$  of RNA were used as input for 3' ligation. During this step, 1  $\mu\text{L}$  of Spike-in (QIAseq miRNA Library QC Spike-in 96, Qiagen, cat#331535; 1:100 dilution) was added. This was followed by the 5' ligation procedure according to the user manual. For reverse transcription, 2  $\mu\text{L}$  of RT initiator was added, and then the procedure was followed as described in the manual. Next, QIAseq miRNA QMN beads were prepared following the user manual and subsequently used for cDNA clean-up. Samples were then frozen at  $-20^{\circ}\text{C}$  overnight. The next day, library amplification was performed using the HT plate indices (Qiagen, cat# 331656) with 22 amplification cycles on a Thermocycler (Nippon Genetics, FastGene

Ultracycler 96, cat# FG-TC01). Afterward, samples were subjected to clean-up using the QMN beads as described above. The supernatant was transferred to a new 96 well polymerase chain reaction (PCR) plate (Nippon Genetics, Semi-Skirted Plates, cat#FG-190250). Subsequently, we followed the clean-up procedure as described in the user manual. 15 µL supernatant was transferred to a new 96 well PCR plate. 1 µL of the samples was used to measure the concentration using Qubit. Another 1 µL was used to run a Bioanalyzer profile (same as above). Based on the Qubit measurement, each sample was adjusted to a concentration of 2 nM cDNA using EB buffer (Qiagen, cat# 19086). Next, the 48 samples were pooled using 2 µL of each sample. After adding 20 µL gel loading dye (New England Biolabs, cat# E6138AA), the pooled samples were run on a 6% TBE PAGE gel (Invitrogen by Thermo Fisher Scientific, cat# EC6265B0X). The gels were run at 145 V, 16 mA for 58 min. For size selection, the region between 165 and 190 bp was cut from the gel. The cut-out was collected in a gel breaker tube placed in a 2 mL tube (IST Engineering Inc., cat# 3388-100) DNA was isolated from the gel according to the "recover purified construct" protocol (5 µL Filter Tubes, IST Engineering Inc., cat# 5388-50) also needed after gel elution described in the QIAseq miRNA Library Kit user manual to obtain 12 µL dsDNA library. The concentration was analyzed via Qubit and bioanalyzer as described above. Small RNA sequencing was performed on an Illumina NextSeq 2000 instrument. For this, the small RNA library pool concentration was adjusted to 2 nM. Loading concentration for the Flow cell was 600 pM. For this dilution is needed in total 25.0 µL: 7.2 µL of the library pool, 16.8 µL RSB with Tween (Illumina) and 1.0 µL PhiX Control (1 nM; NextSeq PhiX Control Kit, cat# FC-110-3002). 20 µL of the diluted sequencing pool was added to the P3 reagent cartridge (NextSeq 2000 P3 reagent, 50 cycles, Illumina, cat #20046810) which was introduced to the sequencer before starting the sequencing cycle according to the user manual.

## 2.4 | Mapping and QC

Illumina's conversion software bcl2fastq (v2.20.2) was used for adapter trimming and converting the base calls in the per-cycle BCL files to the per-read FASTQ format from raw images. QC of raw sequencing data was performed by using FastQC (v0.11.5). Trimming of 3' adapters was done using cutadapt (v1.11.0). The quality of miRNAs reads was evaluated by mirtrace (v1.0.1). Reads were aligned using the mapper.pl script from mirdeep2 (v2.0.1.2) which uses bowtie (v1.1.2) and read counts were generated with the quantifier.pl script from mirdeep2. miRNA annotation was done using miRBase. On average, 8.2mio small RNA reads per sample could be obtained. The average mapping rate was 37%, corresponding to around 3mio miRNA reads per sample. Out of 2876 miRNAs annotated in miRBase, 2154 miRNAs were detected across all samples. As described in Section 2.3, seven "batch control samples" were sequenced in each batch to control for possible intra and inter batch variances. Cross-correlations of replicate samples across all batches show a correlation of  $r > 0.99$  for all samples. In summary, these data indicate almost no variance within and between the 21 batches. Thus, it can be inferred that the miRNA distribution remained stable

during library prep and is independent of sequencing depth. SpikIn cross-correlations were calculated to identify samples with unknown variance from library preparation. From 862 samples, 91% showed SpikIn correlations of  $r > 0.9$ . From the remaining samples, 5% showed correlations of  $r > 0.8$ , 3.3% correlations of  $r > 0.6$ , and 0.7% correlations of  $r < 0.6$ . Samples with high unexplained variance ( $r < 0.6$ ) could be detected in 2 out of 21 batches.

## 2.5 | Statistical analysis

### 2.5.1 | Evaluation of confounding covariates

We used the variancePartition R package<sup>27</sup> to identify covariates that drive the variation in the dataset. The method uses a linear mixed model to partition the variance across multiple known covariates in the data. As expected, the technical covariate batch was identified as the main driver of variation explaining up to 25% of variation in the data. In addition, we included sex and age in the list of unwanted covariates even if their effect on the data seemed to be minor. Our objective was to identify miRNAs for early Alzheimer's risk detection independent of CSF biomarkers or genetic tests, including apolipoprotein E (APOE) status.<sup>28</sup> Therefore, we did not adjust for these covariates to ensure the applicability of our findings in broader screening scenarios. Instead, we used an ordinal regression model to capture the difference in miRNA effect sizes according to APOE status. This model showed that miRNA expression was independent of APOE status. Additionally, a regression model revealed no interaction between the diagnostic group (DXGRP) and APOE status for the majority of the 300 miRNAs in the dataset. In only 24 cases (8%) was the interaction effect significant. Importantly, we confirmed retrospectively that the 15 miRNAs identified as part of signatures for aiding in the identification of EMCI and LMCI patients, as well as their conversion to AD, were not affected by APOE status. Therefore, we conclude that in the context of our miRNA expression data, APOE status is independent of DXGRP in our dataset. Consistent with this, adding APOE status into our different machine learning (ML)-derived miRNA signatures made no difference in predictive power. In none of the different setups did APOE status represent a gain in terms of area under the curve (AUC). Therefore, we conclude that APOE status is largely independent of the miRNA signatures we identified as potential biomarkers in the analyzed dataset.

### 2.5.2 | Data pre-processing

As described in Section 2.3, a total of 2154 miRNAs could be detected across all samples.

Three hundred miRNAs were considered in the subsequent analyses because we removed lowly expressed as well as duplicated miRNAs. More specifically, we included miRNAs in the analysis if they were expressed in at least 95% of the samples with more than 10 reads per sample. Moreover, using small RNA data from plasma, it is not possible to identify the origins of these miRNAs since their mature sequences

are identical. Thus, the reads obtained cannot be attributed to distinct loci; instead, the same number of reads is assigned to each variant from different genomic locations. As a result, read counts represent the overall amount of miRNAs in the plasma samples. To avoid duplicates, we only considered one of the loci variants. Next, data were normalized with DESeq2 (v1.3.40) using the median of ratios method to remove bias of sequencing depth.<sup>29</sup> Size factors were estimated using the poscounts option to consider the zero inflation (~30%) of the data. Unwanted variation from the covariates batch, sex, and age was removed using the RemoveBatchEffect function as implemented in limma (v3.50.3).<sup>30</sup> For ML, the data were standardized using the MaxAbsScaler as implemented in the scikit-learn (v.1.1.2) package.

### 2.5.3 | Linear regression

Regression models were implemented in Python (v3.8.1) using the statsmodels (v.1.1.2) package. Regressions against discrete variables were run using an ordered logistic regression model, whereas for regression against continuous variables a generalized linear model was used. Effects of batch, sex, and age were considered using them as covariates in the regression models.

### 2.5.4 | ML

ML routines were implemented in Python (v3.8.1) using the scikit-learn (v.1.1.2) package. The input dataset was split into training and test set (fraction = 0.3) with random shuffling and in a stratified fashion using the target classes as class labels to ensure that relative class frequencies are preserved in each train and validation run. For cross-validation training the RepeatedStratifiedKFold strategy was used with five splits and three repeats. All random seeds were fixed to ensure reproducibility. Six algorithms from different categories were run for classification.

### 2.5.5 | Detection of miRNA networks

We used inhouse Python scripts to screen interactome databases for annotated interactions using the best miRNA signatures from ML (from miRNAs alone) as input. Results thus obtained contain interactions between input and all (non-)coding genes as annotated in the databases. Interaction information was collected from six different databases: NPInter,<sup>31</sup> RegNetwork,<sup>32</sup> Rise,<sup>33</sup> STRING,<sup>34</sup> TarBase,<sup>35</sup> and TransmiR.<sup>36</sup> ClueGO (2.5.10)<sup>37</sup> was used to conduct pathway analyses and to build networks accordingly.

### 2.5.6 | Selection of miRNA candidates for ML

Potential candidates for ML screening were identified by a two-step approach. First, we included all miRNAs which showed a significant effect size in the regression analyses against diagnosis and conversion.

Second, we ran ML for each miRNA in the dataset to identify the best single miRNA classifiers for the diagnosis. For each condition, the top five miRNAs showing the best AUCs were added resulting in a final list of 73 candidates. miRNA candidates for ML were broken down to a limited list due to runtime considerations. In an ideal case, one would be able to screen all possible combinations for all 300 miRNAs in the dataset. However, such an approach is computationally infeasible given that the total number of combinations to explore is in the order of  $2^{300}$ , where 300 is the amount of detected miRNAs. Therefore, we initially applied a so-called *greedy* strategy<sup>38</sup> to reduce the space of possible combinations that need to be tested. More specifically, we used an iterative procedure where, in each round, the best performing signatures of length  $N$  were selected as seeds based on an AUC threshold to try out new signatures of length  $N+1$  in a subsequent round of the procedure (with  $N$  being the no. of miRNAs). Signatures were extended in each round whereby the no. of miRNAs was successively removed until all remaining miRNAs were tested. However, we noticed that such a strategy did not produce the best results on our data because single miRNAs which showed intermediate performance alone (and were initially dropped out) could become very good predictors when being combined. Therefore, we decided to calculate all possible combinations of one to three miRNAs for our list of 73 candidates and only skip signatures without predictive power ( $AUC \leq 0.5$ ).

## 3 | RESULTS

### 3.1 | Experimental design

The aim of this study was to (1) provide the first blood small RNA sequencing dataset of the ADNI study available for subsequent analysis by the research community, and (2) specifically address whether ML approaches can detect miRNA signatures that aid in the early detection of at-risk patients. We aimed to test the hypothesis that combining plasma miRNA signatures with established approaches for cognitive screening would help identify EMCI and LMCI patients, and predict their conversion to AD. The rationale behind this approach is that neuropsychological testing is generally available. For example, the Mini-Mental State Examination (MMSE) is one of the most widely employed and validated cognitive screening measures for dementia and is often preferred in primary care settings due to its brevity, ease of use, and minimal personnel training requirements, allowing for quick screening of cognitive function. We reasoned that once a miRNA signature is identified through sequencing, subsequent analysis of specific plasma miRNAs can be transferred to simpler assay formats that take only a few hours. This would allow cognitive screening and plasma miRNA analysis to be performed in a primary care setting as a screening approach (Figure 1).

### 3.2 | Detecting plasma miRs in the ADNI study

We carefully selected 847 age- and gender-matched individuals from the ADNI study who, at the time of blood collection, were classified



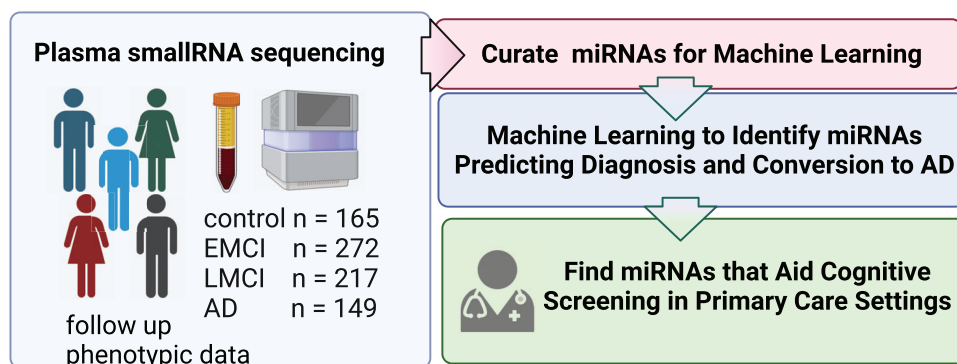


**FIGURE 1** Experimental approach. Schematic overview of the experimental approach to analyze the plasma microRNAome of the Alzheimer's Disease Neuroimaging Initiative (ADNI) study and the overall aim. For further details see text.

as controls, or diagnosed with either EMCI, LMCI, or AD. We ensured that amyloid beta and phosphoTau measures from CSF and neuropsychological testing were available for all individuals. For QC, 15 samples were randomly selected as replicates, leaving us with 862 samples for small RNA sequencing. Small RNA was isolated from plasma samples and library preparation was performed in 21 batches. Spike-in probes were added to each sample before library preparation. Additionally, we added seven control plasma samples prepared according to ADNI SOP to each RNA isolation and sequencing batch for additional QC. These seven samples, referred to as batch control samples, served as internal controls and were processed along with each of the 21 batches, allowing us to control for possible intra- and inter-batch variances. Cross-correlations of these batch control samples showed a correlation coefficient ( $r$ ) of  $>0.99$  for all samples across all batches (Figure 2A). Similar data were obtained when we compared the 15 replicate samples that had been distributed randomly across the 21 batches (Figure 2B). These data indicate almost no variance within and between the 21 batches. Thus, it can be inferred that the miRNA distribution remained stable during library preparation and is independent of sequencing depth. Spike-in cross-correlations were calculated to identify samples with unknown variance from library preparation. Out of 862 samples, 91% showed Spike-in correlations of  $r > 0.9$  (Figure 2C).

We removed 44 samples of "poor" quality ( $r < 0.8$ ) from batch 1 and 7, resulting in 803 samples (control  $n = 165$ ; EMCI  $n = 272$ ; LMCI  $n = 217$ ; AD  $n = 149$ ) for further analysis (Table S1). Our small RNA sequencing identified 300 miRNAs in total and we decided to employ ML classifiers aiming to identify miRNA signatures that could aid in detecting EMCI, LMCI, and AD patients as well as help predicting the conversion of EMCI and LMCI patients to AD. To reduce computing time, thereby allowing us to test for multiple combinations of miRNAs, we first aimed to define a reduced list of miRNAs suitable for ML. For this, after correction for technical confounders and biological covariates, namely batch, age, and sex, we conducted linear regression analyses to test if any of the 300 miRs detected in plasma would correlate with the diagnoses (EMCI, LMCI, or AD). The expression of 23 miRs was positively correlated to the diagnosis (Figure 3A; false discovery rate [FDR]  $< 0.05$ ).

To also capture the miRNAs associated with the conversion of MCI patients to AD, we performed linear regression analyses to test miRNAs versus patients converting from EMCI to AD (EMCI-AD) and from LMCI to AD (LMCI-AD). For the EMCI-AD group, we identified 12 and for the LMCI-AD group 16 significantly correlated miRNAs (Figure 3B). Next, we performed a ML analysis to predict the diagnosis of EMCI, LMCI, MCI, and AD, as well as EMCI-AD and LMCI-AD converters, using all 300 miRNAs detected in our study. It is important to note that in this approach, we did not test for multiple combinations of miRNAs but only analyzed the performance of single miRNAs. From this list, we selected the top five miRNAs and compared this list to the data from the linear regression analysis (Figure 3C). This approach yielded a final list of 73 miRNAs that were subsequently used for all ML analyses.

### 3.3 | ML to predict EMCI, LMCI, and AD

First, ML was applied to find miRNA signatures that could predict the diagnosis of EMCI, LMCI, or AD. In all cases, the best performance was obtained when we combined the expression levels of 3 miRNAs. For AD, a signature of miR.142.3p, miR.98.5p, and miR.9985 yielded an AUC of 0.72 (Figure 4A). Applying the same approach to predict the diagnosis of EMCI, we found miR.590.3p, miR.369.3p, and miR.9985 to predict EMCI patients with an AUC of 0.71 (Figure 4B) and for LMCI a signature consisting of miR.4429, miR.22.5p, and miR.1306 displayed an AUC of 0.71 (Figure 4C). The fact that the expression of different miRNAs indicates MCI (early or late) versus AD is consistent with the notion that the AD pathogenesis is characterized by distinct molecular and cellular phases.<sup>39</sup> These phases are likely governed by specific biological pathways controlled by specific miRNAs. For comparison, we also analyzed the performance of the invasive CSF biomarkers, namely the levels of Abeta42, total Tau (tTAU), phospho-TAU181 (pTAU181), as well as the ratio of Abeta42/tTAU and Abeta42/pTAU181. We first analyzed AD patients. While tTAU (AUC = 0.74) and pTAU181 (AUC = 0.78) performed only slightly better than the miRs, CSF levels of Abeta42 and the Abeta42/tTAU or Abeta42/pTAU181 ratio as well as the MMSE, outperformed the miRNA signature in predicting AD (Figure 4D). This is not unexpected, and it has been suggested that

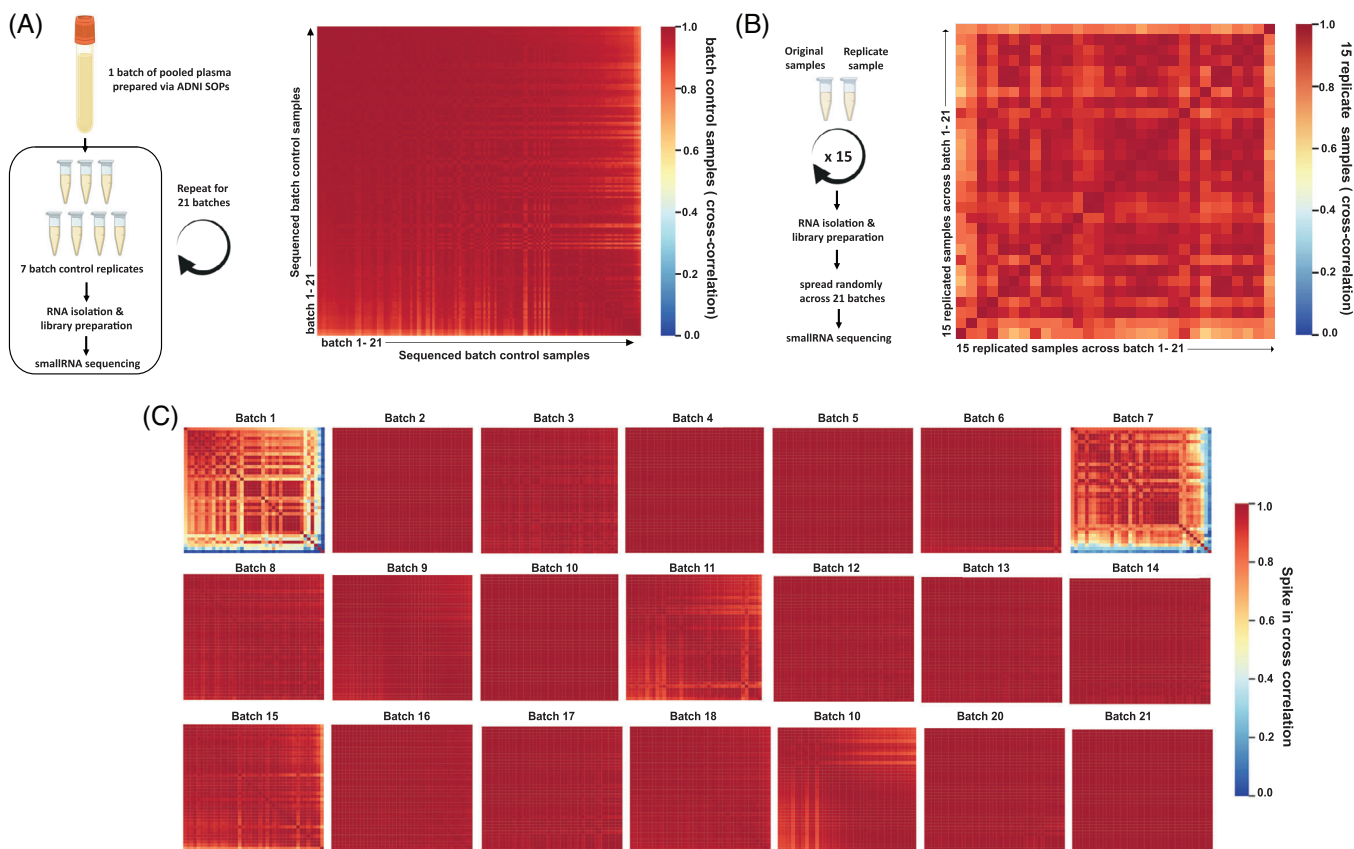


**FIGURE 2** miRNA distribution is largely unaffected by library preparation and independent of sequencing depth. (A) Left panel: experimental design. Right panel: Heatmap showing the cross correlation of the 7 batch control samples across the 21 sequencing batches. (B) Left panel: experimental design. Right panel: Heatmap showing the cross-correlation of the 15 replicated samples that were randomly distributed across the 21 sequencing batches. (C) Heatmaps showing the spike-in cross correlation within each of the 21 sequencing batches. 91% of the samples showed a spike-in cross-correlations of  $r > 0.9$ . Samples with high unknown variance ( $r < 0.6$ ) were detected in batch 1 and 7 and were removed from further analysis resulting in 803 samples in total for the final analysis. miRNA, microRNA.

the most significant impact of analyzing the blood microRNAome is the early detection of patients at risk.<sup>21,40</sup> Indeed, by definition, the MMSE was able to detect AD patients (i.e., late disease) with an AUC of 0.99.

Next, we compared the performance of the miR signature to predict EMCI to those of the CSF biomarkers. In this case, the plasma miRs signature was better than any of the CSF biomarkers (AUC 0.52–0.59) and the MMSE (AUC = 0.64) (Figure 4E). In case of LMCI, the miR signature performed similarly as the levels of CSF biomarkers (AUC = 0.71–0.74) and the MMSE (AUC = 0.73) (Figure 4F).

Combining the three miRNA signatures identified for EMCI with the MMSE data did not further improve the classification of EMCI patients but moderately improved the accuracy to identify LMCI patients from 0.71 to 0.75 (Figure 4G). We also performed a new round of ML analysis using the 73 miRs we had initially selected together with the MMSE data, reasoning that other miRs, beyond those identified when analyzing only miRs, might perform better when combined with MMSE. However, we did not find any combination of three miRs that would further improve the accuracy. In summary, these data suggest that combining the analysis of miRs in plasma could help to detect EMCI and LMCI patients. In conclusion, our findings indicate that the analysis of

miRs in blood plasma could aid the identification of EMCI and LMCI patients and thereby facilitate screening approaches aiming to identify individuals at risk.

### 3.4 | ML to predict the conversion of EMCI and LMCI patients to AD

In addition to finding miRNA-based biomarkers suitable for aiding early diagnostics, there is an urgent need to improve the identification of those MCI patients that will likely develop AD. Follow-up phenotypic data were available for all study participants from the time point of blood collection for up to 144 months. Sixty-nine individuals were excluded from the analysis since they exhibited fluctuating phenotypes, leaving us with 420 MCI patients of which 166 converted to AD. These were 119 LMCI and 47 were EMCI patients (Table S2). Since most of the MCI patients converted within 24 months after baseline assessment (107 out of 166), we simply divided the groups into EMCI and LMCI patients that converted to AD (EMCI-AD; LMCI-AD) and those that did not convert to AD (EMCI-stable;

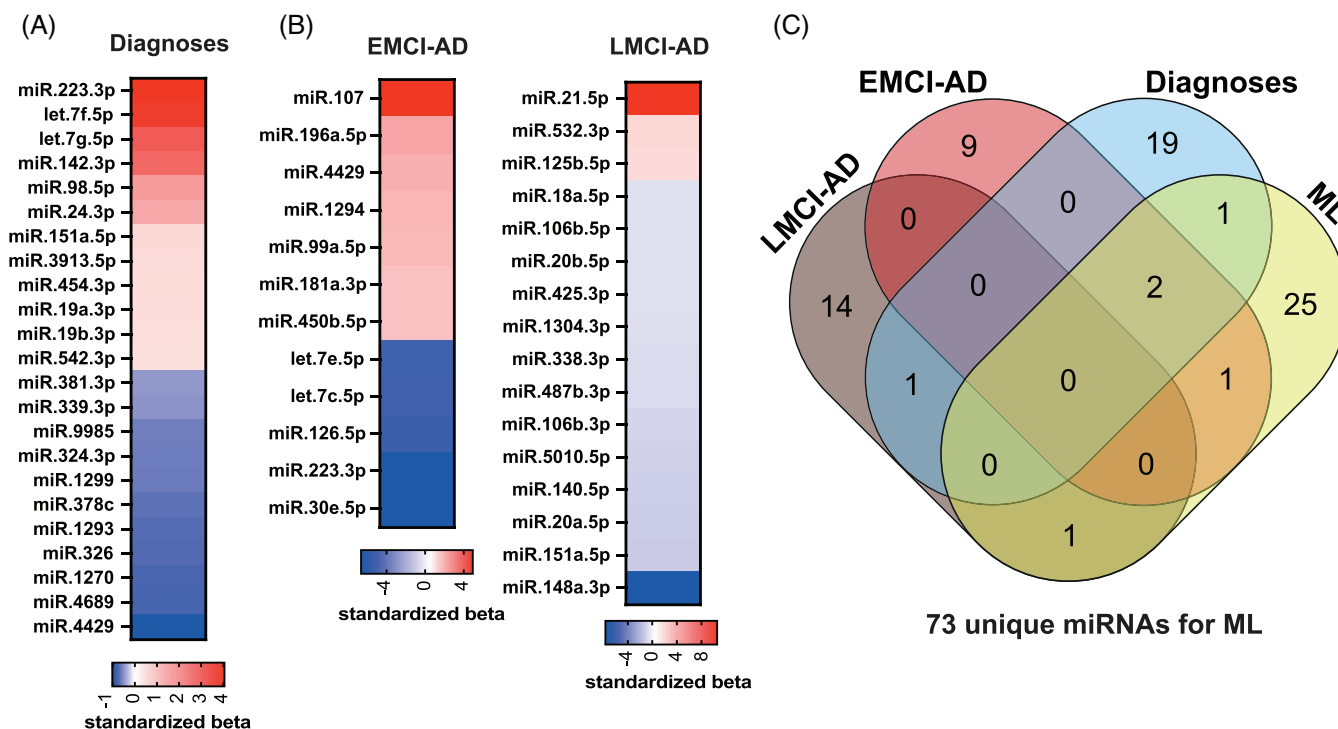


**FIGURE 3** Selecting miRNAs for ML analysis. (A) Heat map showing miRNAs significantly correlated with the diagnostic groups ( $p < 0.05$ , linear regression analysis). (B) Heat map showing miRNAs significantly correlated with EMCI (EMCI-AD) and LMCI (LMCI-AD) patients converting to AD ( $p < 0.05$ , linear regression analysis). (C) Venn diagram comparing the miRNAs significantly correlated to diagnosis, EMCI-AD, LMCI-AD and the top5 miRNAs identified by one round of ML for control vs. EMCI, LMCI, MCI, EMCI-AD, and LMCI-AD revealing 73 unique miRNAs that were subsequently used for all ML approaches. AD, Alzheimer's disease; EMCI, early mild cognitive impairment; LMCI, late mild cognitive impairment; MCI, mild cognitive impairment; miRNA, microRNA; ML, machine learning.

LMCI-stable). First, we employed ML analysis on the EMCI groups and detected a miRNA signature consisting of miR.125b.5p, miR.18a.5p, and miR.26b.5p correctly identifying EMCI-AD conversion with an AUC of 0.70 (Figure 5A), which was better than the performance of the CSF biomarkers (AUC = 0.60–0.62) (Figure 5B). For the LMCI-AD converters a signature combining the expression levels of miR.338.3p, miR.584.5p, and miR.142.3p, was able to detect LMCI-AD patients with an AUC of 0.75 (Figure 5C). Again, the plasma miRNA signature performed better than the CSF biomarkers (Figure 5D).

Of note, the MMSE had no predictive power and failed to identify EMCI-AD or LMCI-AD converters (AUC = 0.5). Therefore, we did not test if combining the MMSE data with miRNA signatures would improve the accuracy. Rather, we decided to employ in this case the ADAScog13 test, which is more comprehensive and detailed than the MMSE. We reasoned that this might still be a suitable screening approach, given that these patients have already received a diagnosis. Thus, this scenario is more likely to occur in a memory clinic than in a primary care setting. Using ML analysis, we observed that ADAScog13 alone was able to predict the conversion from EMCI to AD with an AUC value of 0.57 and those of LMCI patients with 0.65 (Figure 6A,B), which is below the accuracy observed for the miRNA signatures. Combining the identified miRNA signatures with the data of the ADAScog13 was not able to further improve the predictive power over the best scores obtained with the miRNAs alone. To test if other miRNA signatures

may exhibit better performance in combination with the ADAScog13 data, we performed another unbiased ML analysis starting with all 73 miRNAs initially identified. This approach identified a signature consisting of miR.532.3p and miR.1306.3p that was able to predict the conversion of EMCI patients with an AUC value of 0.71 and for LMCI patients with an AUC value of 0.79 which was slightly better than the signature composed of miR.338.3p, miR.584.5p, and miR.142.3p (see Figure 5A,B).

### 3.5 | miRNAs linked to diagnosis and MCI to AD conversion represent specific molecular pathways relevant to AD pathogenesis

As discussed in the Introduction, miRNAs contribute to inter-organ signaling and brain-derived miRNAs can be detected in circulation. It has therefore been suggested that circulating miRNAs may inform about pathological processes in the affected organ including the brain. Therefore, we decided to investigate the molecular pathways controlled by miRNAs identified in our analysis. For this, we selected the miRNA signatures that showed the best performance in detecting EMCI (miR.590.3p, miR.369.3p, miR.9985), LMCI (miR.4429, miR.22.5p, miR.1306), and AD (miR.142.3p, miR.998.5p, miR.9985) as well as those that exhibited the best accuracy to predict



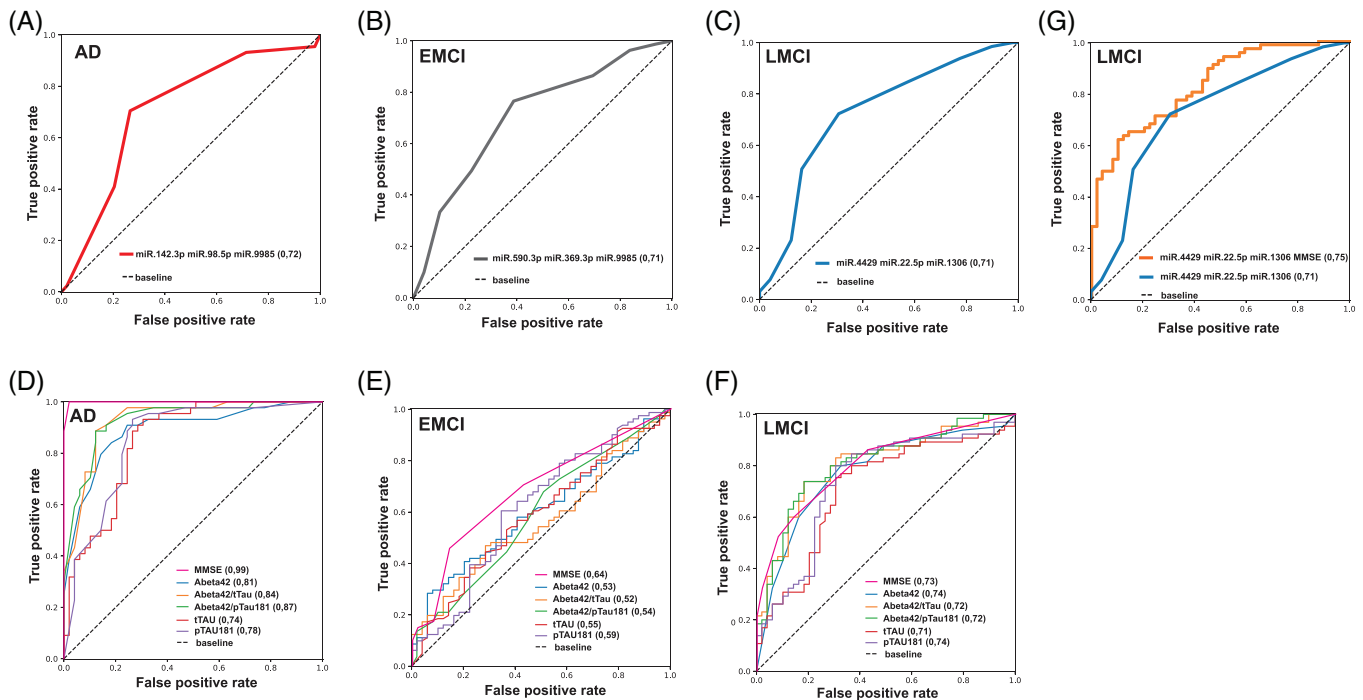


**FIGURE 4** ML identifies miRNA signatures for EMCI, LMCI, and AD. The panels show the results from ML displayed as ROC curve analysis. Numbers in parenthesis indicate the respective AUCs for miRNA predicting AD (A), EMCI (B), or LMCI (C) and for the CSF biomarkers together with MMSE for AD (D), EMCI (E), and LMCI (F). (G) ROC plot showing the results when combining the data for miR-4429, miR-22-5p, and miR-1306 with MMSE. AD, Alzheimer's disease; EMCI, early mild cognitive impairment; LMCI, late mild cognitive impairment; MCI, mild cognitive impairment; miRNA, microRNA; ML, machine learning; MMSE, Mini-Mental State Examination; ROC, receiver operating characteristics.

EMCI (miR.125b.5p, miR.18a.5p, miR.26b.5p) or LMCI (miR.338.3p, miR.548.5p, miR.142.3p) converting to AD. For each of these miRNA signatures we identified confirmed target mRNAs. We further filtered this list for miRNAs expressed in the human brain before proceeding to Gene Ontology (GO) term analysis using ClueGO and Cytoscape to visualize the data. When comparing the results for EMCI, LMCI, and AD, multiple pathways were found across all conditions ( $FDR < 0.05$ ). Among the top 20 pathways observed in all conditions were "Alzheimer's disease" and "Pathways of Neurodegeneration" (Figure 7, Table S3). Interestingly, several pathways were specific to EMCI and LMCI. For example, "Ferroptosis", "Necroptosis", "Retrograde endocannabinoid signaling", "Oxidative phosphorylation", "JAK-STAT signaling pathway", "p53 signaling", and "MicroRNAs in cancer" were exclusively observed in EMCI patient (Figure 7, Table S3). For LMCI we detected 28 unique pathways that included those linked to inflammatory processes such as "IL-17 signaling pathway" and "Natural killer cell mediated cytotoxicity", "B cell receptor signaling pathway", and "C-type lectin receptor signaling pathway", pathways linked to cognitive processes such as "Cholinergic synapse" and "cAMP signaling pathway" or "Amphetamine addiction" or "Estrogen signaling pathway", pathways linked to mitochondria dysfunction, namely "Mitophagy" and pathways that may hint to a de-regulation of vascular processes such as "Platelet activation", "Aldosterone-regulated sodium reabsorption", "Endocrine and other factor-regulated calcium reabsorption", "Vasopressin-regulated water reabsorption" "Gap junction", and "Carbohydrate digestion and absorption" (Figure 7, Table

S3). We did not observe any pathways exclusive to AD. In addition to the already mentioned pathways "Alzheimer's disease" and "Pathways of Neurodegeneration" within the top 20 pathways linked to AD we identified, for example, the ErbB signaling pathway that was also a main target of miRNAs that correlate with A/T/N positivity (Liu et al., under review in *Alzheimer's & Dementia*). Additional pathways identified included "AMPK signaling pathway", "HIF-1 signaling pathway", "Autophagy", "mRNA surveillance pathway", "RNA degradation", "Long-term depression", and "Chemokine signaling pathway" (Figure 7, Table S3).

Using similar approach, we sought to identify molecular pathways controlled by miRNAs found to associate with EMCI-AD (miR.125b.5p, miR.18a.5p, miR.26b.5p) and LMCI-AD (miR.338.3p, miR.584.5p, miR.142.3p) progression. We identified 59 pathways ( $FDR < 0.05$ ) that were common to EMCI-AD and LMCI-AD converters. These included pathways linked to neuronal plasticity such as "Axon guidance" and pathways related to neurodegenerative process such as "Alzheimer disease", "HIF-1 signaling pathway", "Ubiquitin mediated proteolysis", "Autophagy", and "Apoptosis", pathways linked to viral infection and inflammatory processes such as "Fc gamma R-mediated phagocytosis", "Human cytomegalovirus infection", "Pathogenic Escherichia coli infection", "Viral life cycle", metabolic processes including "N-Glycan biosynthesis", and "Sphingolipid signaling pathway" as well as pathways suggesting vascular pathology, for example, "Lipid and atherosclerosis" and "Fluid shear stress and atherosclerosis" (Figure 8, Table S4).

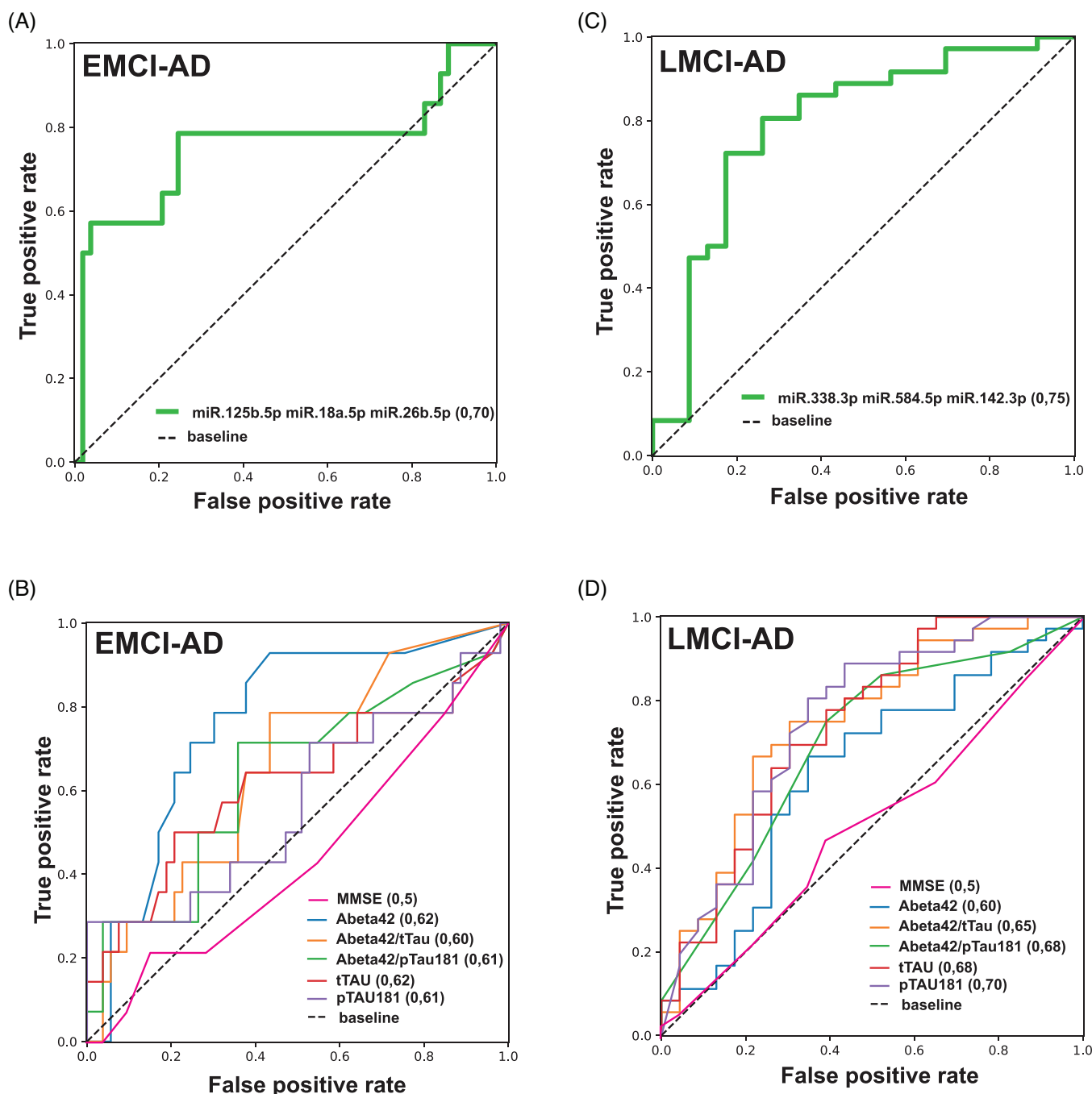


**FIGURE 5** ML identifies miRNA signatures to predict EMCI-AD and LMCI-AD converters. (A) ROC curve displaying the results from ML using miR.125b.5p, miR.18a.3p and miR.25b.5p predicting EMCI-AD converters with an AUC of 0.70. (B) ROC curve showing the performance of MMSE and CSF biomarkers to identify EMCI-AD converters. (C) ROC curve showing that a signature of miR.338.3p, miR.584.5p and miR.142.3p can predict LMCI-AD converters with an AUC of 0.75. (D) ROC curve showing the performance of MMSE and CSF biomarkers to identify LMCI-AD converters. Numbers in parenthesis indicate the respective AUC values. AD, Alzheimer's disease; AUC, area under the curve; CSF, cerebrospinal fluid; EMCI, early mild cognitive impairment; LMCI, late mild cognitive impairment; MCI, mild cognitive impairment; miRNA, microRNA; ML, machine learning; MMSE, Mini-Mental State Examination; ROC, receiver operating characteristics.

Seven pathways were specific to LMCI-AD these were linked to neurodegeneration and inflammation, namely "Pathways of neurodegeneration" and "TGF-beta signaling pathway", while the other pathways exclusively detected in LMCI-converters were "Estrogen signaling pathway" and pathways representing metabolic processes

including "Glycerolipid metabolism", "Arginine and proline metabolism", "Steroid biosynthesis", and "Fatty acid biosynthesis" (Figure 8). Sixty-four pathways were specific to EMCI-AD converters. These included pathways linked to synaptic plasticity such as "Synaptic vesicle cycle", "Neurotrophin signaling pathway", and "Long-term

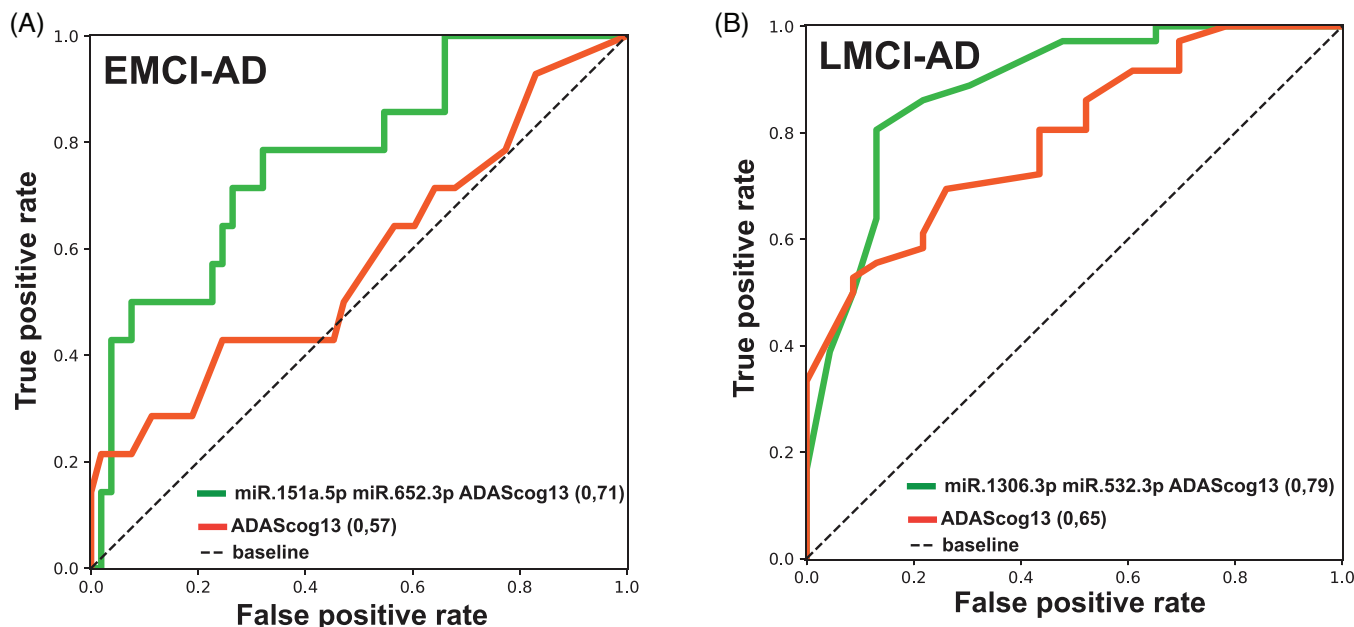


**FIGURE 6** ML-identified miRNA signatures to predict EMCI-AD and LMCI-AD converters in combination with the ADAScog13 test. (A) ROC curve displaying the results from ML using miR.151a.5p and miR.652.3p in combination with the ADAScog13 test predicting EMCI-AD converters. (B) ROC curve showing the performance of miR.1306.3p and miR.532.3p in combination with the ADAScog13 test to predict LMCI-AD converters. Numbers in parenthesis indicate the respective AUC values. AD, Alzheimer's disease; EMCI, early mild cognitive impairment; LMCI, late mild cognitive impairment; MCI, mild cognitive impairment; miRNA, microRNA; ML, machine learning; MMSE, Mini-Mental State Examination; ROC, receiver operating characteristics.

potentiation". We also detected pathways linked to vascular function such as "Vasopressin-regulated water reabsorption", "Apelin signaling pathway", and "Aldosterone-regulated sodium reabsorption". In addition to pathways that represent response to viral and bacterial infection and inflammation, for example, "Herpes simplex virus 1 infection", "Chemokine signaling pathway", we detected "Mitophagy" and "Oxidative phosphorylation" which may suggest deregulated mitochondria function in EMCI-AD converters. It is interesting to note that "Mitophagy" was also detected as a pathway specific to patients with the LMCI diagnosis that was not observed in EMCI patients, which might help to explain why some EMCI patients convert to AD, while others remain stable.

## 4 | DISCUSSION

We present the first small RNA sequencing data from plasma samples of ADNI study participants, providing a valuable resource for the field and exploring whether ML can identify miRNA signatures to be utilized in early detection of individuals at-risk for developing AD-associated cognitive decline. Specifically, we hypothesized that analyzing plasma miRNA in combination with cognitive screening could help early diagnosis of MCI and, importantly, predict which MCI patients will progress toward AD.

Out of the 300 miRNAs reliably detected in plasma samples across individuals, we identified 15 miRNAs that were associated with AD, or helped detect EMCI and LMCI patients, or predicted their conver-

sion to AD. Notably, 13 of these miRNAs had previously been found deregulated in AD when analyzed in various blood components such as whole blood, serum, plasma, or blood-derived extracellular vesicles (EVs). Although these previous datasets analyzed fewer samples and mainly focused on AD rather than MCI patients or MCI-to-AD converters, the fact that our findings support previous reports attest to the quality of our dataset.

We detected a signature consisting of miR.142.3p, miR.98.5p, and miR.9985 to identify AD patients with an AUC value of 0.72. Although our primary goal was not to identify AD patients—since neuropsychological testing and CSF biomarkers offer much greater accuracy—it is interesting to note that miR.142.3p was deregulated in whole blood or serum-derived EVs from AD patients analyzed via RNA sequencing.<sup>41,42</sup> Notably, in our dataset, miR.142.3p was also part of the miRNA signature to identify LMCI-AD converters. Moreover, miR.142.3p was found to be upregulated in the hippocampus of AD patients,<sup>43</sup> and SNPs in the miR.142 promoter have been associated with reduced AD risk.<sup>44</sup> Functional studies have shown that miR.142.3p is involved in the downregulation of BDNF in activated microglia, suggesting it may play a role in microglia-neuron cross talk in AD.<sup>45</sup> Similarly, miR.98.5p has been implicated in the pathophysiology of AD<sup>46</sup> and was found to be deregulated in whole blood<sup>41</sup> and serum samples of AD patients.<sup>47</sup> Finally, miR.9985 was reported as upregulated in serum EVs of AD patients.<sup>42</sup>

Perhaps more interesting than miRNAs associated with AD are the miRNAs that aid in EMCI diagnosis and the detection of individuals at risk. Notably, miR.9985 was part of a signature, together

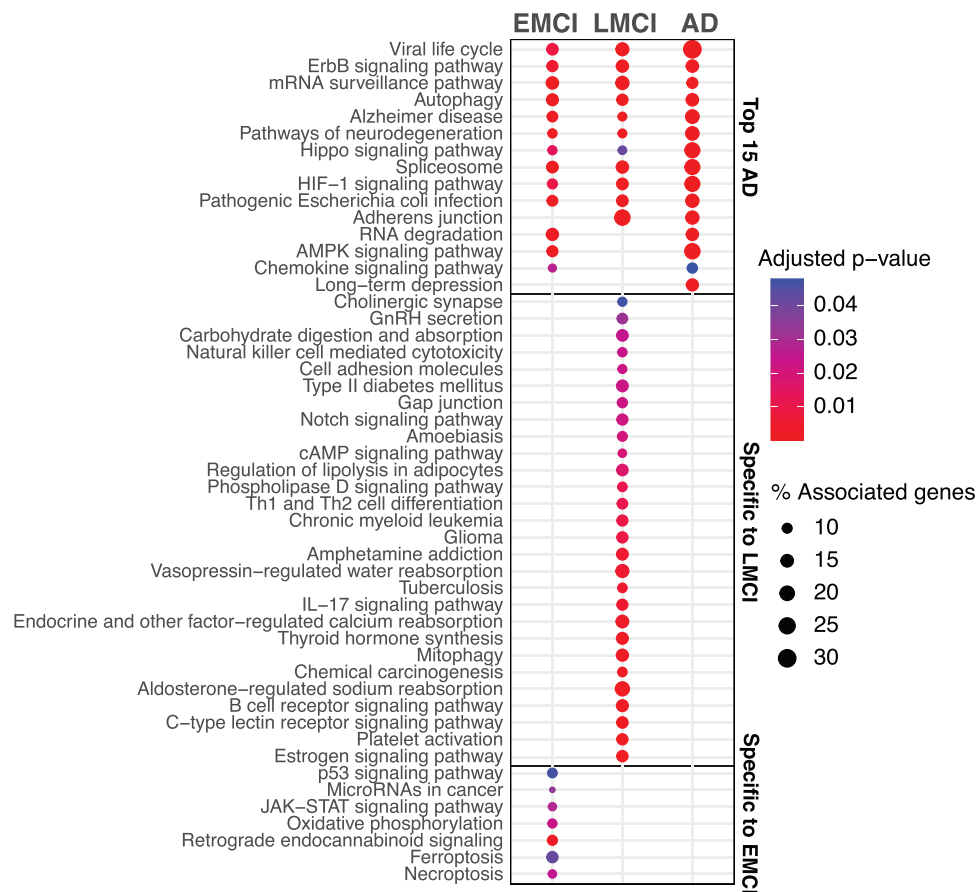


**FIGURE 7** Pathways controlled by miRNAs associated with EMCI, LMCI, and AD. Dot plot showing the top 15 pathways affected in AD, as well as the pathways specific to the LMCI, AD across diagnoses. AD, Alzheimer's disease; EMCI, early mild cognitive impairment; LMCI, late mild cognitive impairment; miRNA, microRNA.

with miR.590.3p and miR.369.3p, which identified EMCI patients with greater accuracy than CSF biomarkers or MMSE scores. Like miR.9985, miR.590.3p was reported to be deregulated in serum and plasma EVs,<sup>42</sup> and miR.369.3p has been associated with AD pathology.<sup>48</sup>

LMCI patients were identified with an AUC of 0.71 when combining miR.4429, miR.22.5p, and miR.1306. While miR.4429 has not been associated with AD, it was found to be a blood biomarker in schizophrenia.<sup>49</sup> miR.22.5p was deregulated in blood samples from AD patients<sup>50</sup> and has been described as part of an Immunity-Associated Regulatory Network in AD.<sup>51</sup> miR.1306 expression differences were observed when whole blood samples of AD patients were compared to controls.<sup>52,53</sup>

Equally important as the early identification of at-risk individuals is predicting who will convert from MCI to AD. A signature consisting of miR.125b.5p, miR.18a.5p, and miR.26a.5p was able to predict EMCI-AD converters with an AUC of 0.7, which was superior to the performance of the invasive CSF biomarkers and the MMSE. All three miRNAs were reported to differ in AD patients in whole blood, plasma, serum, and plasma EVs.<sup>54-58</sup> Functionally, miR.125b.5p is known to regulate synaptic plasticity and its overexpression is associated with memory deficits and tau hyperphosphorylation.<sup>59</sup> Similarly, miR.26b.5p targets Retinoblastoma protein, which leads to

aberrant cell cycle entry, cyclin-dependent kinase 5 upregulation, and subsequent tau phosphorylation and cell death in AD.<sup>60</sup>

For predicting LMCI-AD, we identified a signature consisting of miR.338.3p, miR.584.5p, and miR.142.3p, which demonstrated greater accuracy than the CSF biomarker and MMSE. Both miR.338.3p and miR.584.5p have been identified as blood biomarkers for AD when analyzing whole blood, plasma, or plasma EVs.<sup>41,55,61</sup> Additionally, the miRNA signature miR.151.5p, miR.652.3p and the microRNA signature miR.1306.3p, miR.532.3p improved the prediction of conversions from EMCI to AD and from LMCI to AD, respectively. While there are no data reporting deregulation of miR.151.5p in AD, it has been identified in whole blood samples from soccer players with mild traumatic brain injury.<sup>62</sup> Similarly, while little is known about miR.652.3p, recent studies reported altered levels of miR.652.3p in blood associated with Internet gaming disorder<sup>63</sup> and attention deficit hyperactivity disorder (ADHD).<sup>64</sup> miR.1306.5p was also part of the signature to detect LMCI, and miR.532.3p was found to be deregulated in serum samples from AD patients.<sup>56</sup>

In summary, these data strongly support the significance of the identified miRNAs in developing novel biomarkers for detecting at-risk patients in the context of AD. It is noteworthy that while some studies found these miRNAs to be up regulated in AD, others reported



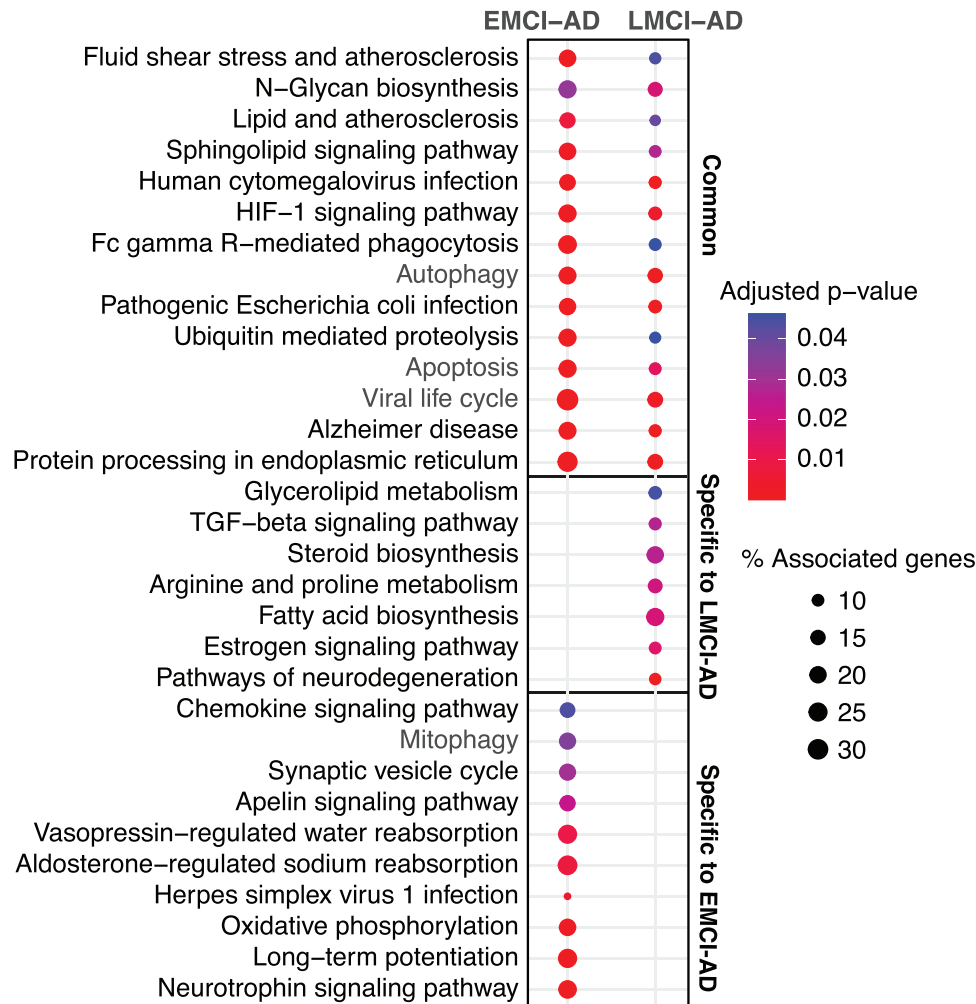


**FIGURE 8** Pathways controlled by miRNAs associated with EMCI-AD and LMCI-AD converters. Dot plot showing the top common pathways affected in EMCI-AD and LMCI-AD, as well as the pathways specific to each condition. AD, Alzheimer's disease; EMCI, early mild cognitive impairment; LMCI, late mild cognitive impairment; miRNA, microRNA.

the opposite. This might underscore the importance of analyzing different phases of AD progression, such as EMCI, LMCI, and AD, and relying on ML approaches to analyze miRNA signatures rather than measuring the up- or down-regulation of single miRNAs. Our hypothesis that circulating miRNA signatures could capture different phases in the development of AD is supported by the corresponding confirmed mRNA target genes. While interpreting such data requires caution since we extrapolate circulating miRNA signatures to molecular changes in the brain, our findings suggest that the miRNA signatures detecting EMCI, LMCI, or AD represent distinct molecular processes. For instance, pathways exclusively associated with either EMCI or LMCI were identified. Specifically, the miRNA signature linked to EMCI was associated with processes such as ferroptosis and oxidative phosphorylation, consistent with data suggesting that deregulated iron and energy metabolism are early events in AD pathogenesis.<sup>65,66</sup> In contrast, only in the LMCI signature did we observed processes hinting at vascular damage and interleukin-17 signaling, which have been associated with AD progression.<sup>39,67</sup> It is plausible to speculate that developing plasma miRNA signatures could enable the

specific detection of distinct phases of AD, thus improving diagnostic ability.

Our study has a few limitations that should be considered. First, this is an observational study, with predominantly non-Hispanic White participants. Therefore, it will be important to investigate populations with greater diversity to determine if our results translate to other ethnic groups or if other groups are characterized by additional miRNA dementia-related biomarkers. Second, the diagnostic groups analyzed here were based on clinical criteria and no neuropathologic confirmation was possible in this *ante mortem* study, though we used several AD-related endophenotypes such as CSF biomarkers to address this limitation. Third, our study is cross-sectional. It would be valuable to perform similar studies in a longitudinal fashion to determine the trajectories of microRNAs as biomarkers over time. Fourth, the observed associations between plasma microRNAs and our dementia-related measures could have been influenced by environmental or genetic factors not considered in the current analysis. Fifth, as in any observational study, we cannot establish if the associations detected are causal in nature.

Overall, this study represents a significant step forward in understanding the potential of plasma microRNA signatures as prognostic AD biomarkers. By providing the first blood small RNA sequencing dataset of the ADNI study, we have laid the groundwork for further investigations into the role of microRNAs in AD pathogenesis. Future research should refine and confirm the reported miRNA signatures. We envision that, once specific miRNA signatures are established and confirmed, the analysis of blood miRNAs will be transferred from labor and cost intensive sequencing approaches used in our study to simpler assay formats. This will open avenues toward adopting blood miRNAome analysis in clinical practice. Integrating plasma microRNA signatures with established cognitive screening measures in primary care settings will likely enhance the accuracy and efficiency of recognizing early AD-associated cognitive decline.

## ACKNOWLEDGMENTS

We are grateful to the ADNI participants and the ADNI staff who made the samples available for this study. This work was supported by NIH RF1AG078299, AG067188, ADNI4, P30PENNADRC, R01AG080670, P30AG073107, P30AG072978, U19AG068753 (I. Delalle, J.K. Blusztajn, A. Fischer, A. Saykin, K. Nho, H. Lin, A.L. DeStefano, A. Kronic); NIH U19AG024904, P30AG072976, and U19AG074879 provide funding for A. Saykin (also supported by NIH P30AG010133, R01AG019771, R01AG057739, R01LM013463, R01AG068193, T32AG071444, U01AG068057), K. Nho (also supported by NIH U01AG072177), S. Lui, T. Park, Y-N Huang Y-N, and S.L. Risacher; NIH RF1AG057768, P30AG013846, RF1AG072654 (J.K. Blusztajn); NIH U01AG068221-01A1 (H. Lin and A.L. DeStefano); NIH U01AG058589, R01DK122503 (A.L. DeStefano); Alzheimer's Association AARG-NTF-20-643020 (H. Lin); American Heart Association 20SFRN35460034 (H. Lin); the DFG (Deutsche Forschungsgemeinschaft) Priority Program 1738, SFB1286 and GRK2824; the German Federal Ministry of Science and Education (BMBF) via the ERA-NET Neuron Project EPINEURODEVO; the EU Joint Programme-Neurodegenerative Diseases (JPND)—EPI-3E; Germany's Excellence Strategy—EXC 2067/1 390729940 (A. Fischer, D.M. Krueger, T. Pena, R. Pradhan, S. Burkhardt, R. Schroeder, N. Hempel); GoBio Project miRassay (16LW0055) by the German Federal Ministry of Science and Education (F. Sananbenesi, A. Schutz). The above funding sources had no role in study design, collection, analysis, and interpretation of data, writing of the manuscript, or the decision to submit the article for publication.

## CONFLICT OF INTEREST STATEMENT

The authors declare no conflicts of interest. Author disclosures are available in the [Supporting information](#).

## CONSENT STATEMENT

Informed consent was obtained from all participants.

## ORCID

Ivana Delalle  <https://orcid.org/0000-0002-1873-3064>

## REFERENCES

- Bateman RJ, Xiong C, Benzinger TL, et al. Clinical and biomarker changes in dominantly inherited Alzheimer's disease. *N Engl J Med*. 2012;367(9):795-804. doi:10.1056/NEJMoa1202753
- Schneider LS, Mangialasche F, Andreasen N, et al. Clinical trials and late-stage drug development for Alzheimer's disease: An appraisal from 1984 to 2014. *J Intern Med*. 2014;275(3):251-283. doi:10.1111/joim.12191
- Bucci M, Chiotis K, Nordberg A. Alzheimer's Disease Neuroimaging I. Alzheimer's disease profiled by fluid and imaging markers: Tau PET best predicts cognitive decline. *Mol Psychiatry*. 2021;26(10):5888-5898. doi:10.1038/s41380-021-01263-2
- Dubois B, Feldman HH, Jacova C, et al. Advancing research diagnostic criteria for Alzheimer's disease: The IWG-2 criteria. *Lancet Neurol*. 2014;13(6):614-629. doi:10.1016/S1474-4422(14)70090-0
- Therriault J, Schindler SE, Salvado G, et al. Biomarker-based staging of Alzheimer disease: Rationale and clinical applications. *Nat Rev Neurol*. 2024;20(4):232-244. doi:10.1038/s41582-024-00942-2
- Olsson B, Lautner R, Andreasson U, et al. CSF and blood biomarkers for the diagnosis of Alzheimer's disease: A systematic review and meta-analysis. *Lancet Neurol*. 2016;15(7):673-684. doi:10.1016/S1474-4422(16)00070-3
- Blennow K. A review of fluid biomarkers for Alzheimer's disease: Moving from CSF to blood. *Neurol Ther*. 2017;6(Suppl 1):15-24. doi:10.1007/s40120-017-0073-9
- Li D, Mielke MM. An update on blood-based markers of Alzheimer's disease using the SiMoA platform. *Neurol Ther*. 2019;8(Suppl 1):73-82. doi:10.1007/s40120-019-00164-5
- Montoliu-Gaya L, Alosco ML, Yhang E, et al. Optimal blood tau species for the detection of Alzheimer's disease neuropathology: An immunoprecipitation mass spectrometry and autopsy study. *Acta Neuropathol*. 2023;147(1):5. doi:10.1007/s00401-023-02660-3
- Gurtan AM, Sharp PA. The role of miRNAs in regulating gene expression networks. *J Mol Biol*. 2013;425(19):3582-3600. doi:10.1016/j.jmb.2013.03.007
- Zampetaki A, Mayr M. MicroRNAs in vascular and metabolic disease. *Circ Res*. 2012;110(3):508-522. doi:10.1161/CIRCRESAHA.111.247445
- Condrat CE, Thompson DC, Barbu MG, et al. miRNAs as biomarkers in disease: Latest findings regarding their role in diagnosis and prognosis. *Cells*. 2020;9(2):276. doi:10.3390/cells9020276
- Bayraktar R, Van Roosbroeck K, Calin GA. Cell-to-cell communication: MicroRNAs as hormones. *Mol Oncol*. 2017;11(12):1673-1686. doi:10.1002/1878-0261.12144
- Jose AM. Movement of regulatory RNA between animal cells. *Genesis*. 2015;53(7):395-416. doi:10.1002/dvg.22871
- Mustapic M, Eitan E. Plasma extracellular vesicles enriched for neuronal origin: A potential window into brain pathologic processes. *Front Neurosci*. 2017;11:278. doi:10.3389/fnins.2017.00278
- Cortez MA, Bueso-Ramos C, Ferdin J, Lopez-Berestein G, Sood AK, Calin GA. MicroRNAs in body fluids—the mix of hormones and biomarkers. *Nat Rev Clin Oncol*. 2011;8(8):467-477. doi:10.1038/nrclinonc.2011.76
- Rao P, Benito E, Fischer A. MicroRNAs as biomarkers for CNS disease. *Front Mol Neurosci*. 2013;6:39. doi:10.3389/fnmol.2013.00039
- Galimberti D, Villa C, Fenoglio C, et al. Circulating miRNAs as potential biomarkers in Alzheimer's disease. *J Alzheimers Dis*. 2014;42(4):1261-1267. doi:10.3233/JAD-140756
- Mitchell PS, Parkin RK, Kroh EM, et al. Circulating microRNAs as stable blood-based markers for cancer detection. *Proc Natl Acad Sci U S A*. 2008;105(30):10513-10518. doi:10.1073/pnas.0804549105
- Sandau US, Wiedrick JT, McFarland TJ, et al. Analysis of the longitudinal stability of human plasma miRNAs and implications for disease biomarkers. *Sci Rep*. 2024;14(1):2148. doi:10.1038/s41598-024-52681-5

21. Islam MR, Kaurani L, Berulava T, et al. A microRNA signature that correlates with cognition and is a target against cognitive decline. *EMBO Mol Med*. 2021;13(11):e13659. doi:10.15252/emmm.202013659
22. Walgrave H, Zhou L, De Strooper B, Salta E. The promise of microRNA-based therapies in Alzheimer's disease: Challenges and perspectives. *Mol Neurodegener*. 2021;16(1):76. doi:10.1186/s13024-021-00496-7
23. Kanach C, Blusztajn JK, Fischer A, Delalle I. MicroRNAs as candidate biomarkers for Alzheimer's disease. *Noncoding RNA*. 2021;7(1):8. doi:10.3390/nrna7010008
24. Weiner MW, Veitch DP, Aisen PS, et al. Impact of the Alzheimer's Disease Neuroimaging Initiative, 2004 to 2014. *Alzheimers Dement*. 2015;11(7):865-884. doi:10.1016/j.jalz.2015.04.005
25. Saykin AJ, Shen L, Yao X, et al. Genetic studies of quantitative MCI and AD phenotypes in ADNI: Progress, opportunities, and plans. *Alzheimers Dement*. 2015;11(7):792-814. doi:10.1016/j.jalz.2015.05.009
26. Veitch DP, Weiner MW, Miller M, et al. The Alzheimer's Disease Neuroimaging Initiative in the era of Alzheimer's disease treatment: A review of ADNI studies from 2021 to 2022. *Alzheimers Dement*. 2024;20(1):652-694. doi:10.1002/alz.13449
27. Hoffman GE, Schadt EE. variancePartition: Interpreting drivers of variation in complex gene expression studies. *BMC Bioinformatics*. 2016;17(1):483. doi:10.1186/s12859-016-1323-z
28. Risacher SL, Kim S, Shen L, et al. The role of apolipoprotein E (APOE) genotype in early mild cognitive impairment (E-MCI). *Front Aging Neurosci*. 2013;5:11. doi:10.3389/fnagi.2013.00011
29. Love MI, Huber W, Anders S. Moderated estimation of fold change and dispersion for RNA-seq data with DESeq2. *Genome Biol*. 2014;15(12):550. doi:10.1186/s13059-014-0550-8
30. Ritchie ME, Phipson B, Wu D, et al. limma powers differential expression analyses for RNA-sequencing and microarray studies. *Nucleic Acids Res*. 2015;43(7):e47. doi:10.1093/nar/gkv007
31. Teng X, Chen X, Xue H, et al. NPInter v4.0: An integrated database of ncRNA interactions. *Nucleic Acids Res*. 2020;48(D1):D160-D165. doi:10.1093/nar/gkz969
32. Liu ZP, Wu C, Miao H, Wu H. RegNetwork: An integrated database of transcriptional and post-transcriptional regulatory networks in human and mouse. *Database (Oxford)*. 2015;2015:bav095. doi:10.1093/database/bav095
33. Gong J, Shao D, Xu K, et al. RISE: A database of RNA interactome from sequencing experiments. *Nucleic Acids Res*. 2018;46(D1):D194-D201. doi:10.1093/nar/gkx864
34. Szklarczyk D, Gable AL, Lyon D, et al. STRING v11: Protein-protein association networks with increased coverage, supporting functional discovery in genome-wide experimental datasets. *Nucleic Acids Res*. 2019;47(D1):D607-D613. doi:10.1093/nar/gky1131
35. Karagkouni D, Paraskevopoulou MD, Chatzopoulos S, et al. DIANA-TarBase v8: A decade-long collection of experimentally supported miRNA-gene interactions. *Nucleic Acids Res*. 2018;46(D1):D239-D245. doi:10.1093/nar/gkx1141
36. Tong Z, Cui Q, Wang J, Zhou Y. TransmiR v2.0: An updated transcription factor-microRNA regulation database. *Nucleic Acids Res*. 2019;47(D1):D253-D258. doi:10.1093/nar/gky1023
37. Bindea G, Mlecnik B, Hackl H, et al. ClueGO: A Cytoscape plug-in to decipher functionally grouped gene ontology and pathway annotation networks. *Bioinformatics*. 2009;25(8):1091-1093. doi:10.1093/bioinformatics/btp101
38. Borboudakis G, Tsamardinos I. Extending greedy feature selection algorithms to multiple solutions. *Data Min Knowl Discov*. 2021;35(4):1393-1434. doi:10.1007/s10618-020-00731-7
39. De Strooper B, Karran E. The cellular phase of Alzheimer's disease. *Cell*. 2016;164(4):603-615. doi:10.1016/j.cell.2015.12.056
40. Salta E, De Strooper B. Noncoding RNAs in neurodegeneration. *Nat Rev Neurosci*. 2017;18(10):627-640. doi:10.1038/nrn.2017.90
41. Keller A, Backes C, Haas J, et al. Validating Alzheimer's disease micro RNAs using next-generation sequencing. *Alzheimers Dement*. 2016;12(5):565-576. doi:10.1016/j.jalz.2015.12.012
42. Chen SD, Huang YY, Shen XN, et al. Longitudinal plasma phosphorylated tau 181 tracks disease progression in Alzheimer's disease. *Transl Psychiatry*. 2021;11(1):356. doi:10.1038/s41398-021-01476-7
43. Lau P, Bossers K, Janky R, et al. Alteration of the microRNA network during the progression of Alzheimer's disease. *EMBO Mol Med*. 2013;5(10):1613-1634. doi:10.1002/emmm.201201974
44. Ghanbari M, Munshi ST, Ma B, et al. A functional variant in the miR-142 promoter modulating its expression and conferring risk of Alzheimer disease. *Hum Mutat*. 2019;40(11):2131-2145. doi:10.1002/humu.23872
45. Gupta N, Jadhav S, Tan KL, Saw G, Mallilankaraman KB, Dheen ST. miR-142-3p regulates BDNF expression in activated rodent microglia through its target CAMK2A. *Front Cell Neurosci*. 2020;14:132. doi:10.3389/fncel.2020.00132
46. Li Q, Li X, Wang L, Zhang Y, Chen L. miR-98-5p acts as a target for Alzheimer's disease by regulating abeta production through modulating SNX6 expression. *J Mol Neurosci*. 2016;60(4):413-420. doi:10.1007/s12031-016-0815-7
47. Aksoy-Aksel A, Zampa F, Schrott G. MicroRNAs and synaptic plasticity—a mutual relationship. *Philos Trans R Soc Lond B Biol Sci*. 2014;369(1652):20130515. doi:10.1098/rstb.2013.0515
48. Yao X, Xian X, Fang M, Fan S, Li W. Loss of miR-369 promotes tau phosphorylation by targeting the Fyn and serine/threonine-protein kinase 2 signaling pathways in Alzheimer's disease mice. *Front Aging Neurosci*. 2019;11:365. doi:10.3389/fnagi.2019.00365
49. Davarinejad O, Najafi S, Zhaleh H, et al. MiR-574-5P, miR-1827, and miR-4429 as potential biomarkers for schizophrenia. *J Mol Neurosci*. 2022;72(2):226-238. doi:10.1007/s12031-021-01945-0
50. Dakterzade F, Targa A, Benitez ID, et al. Identification and validation of endogenous control miRNAs in plasma samples for normalization of qPCR data for Alzheimer's disease. *Alzheimers Res Ther*. 2020;12(1):163. doi:10.1186/s13195-020-00735-x
51. Wu Z, Dong L, Tian Z, et al. Integrative analysis of the age-related dysregulated genes reveals an inflammation and immunity-associated regulatory network in Alzheimer's disease. *Mol Neurobiol*. 2024;61(8):5353-5368. doi:10.1007/s12035-023-03900-z
52. Pichler S, Gu W, Hartl D, et al. The miRNome of Alzheimer's disease: Consistent downregulation of the miR-132/212 cluster. *Neurobiol Aging*. 2017;50:167.e1-167 e10. doi:10.1016/j.neurobiolaging.2016.09.019
53. Wu Y, Xu J, Xu J, et al. Lower serum levels of miR-29c-3p and miR-19b-3p as biomarkers for Alzheimer's disease. *Tohoku J Exp Med*. 2017;242(2):129-136. doi:10.1620/tjem.242.129
54. Dong Z, Gu H, Guo Q, et al. Profiling of serum exosome MiRNA reveals the potential of a MiRNA panel as diagnostic biomarker for Alzheimer's disease. *Mol Neurobiol*. 2021;58(7):3084-3094. doi:10.1007/s12035-021-02323-y
55. Lugli G, Cohen AM, Bennett DA, et al. Plasma exosomal miRNAs in persons with and without Alzheimer disease: Altered expression and prospects for biomarkers. *PLoS One*. 2015;10(10):e0139233. doi:10.1371/journal.pone.0139233
56. Tan L, Yu JT, Tan MS, et al. Genome-wide serum microRNA expression profiling identifies serum biomarkers for Alzheimer's disease. *J Alzheimers Dis*. 2014;40(4):1017-1027. doi:10.3233/JAD-132144
57. Leidinger P, Backes C, Deutscher S, et al. A blood based 12-miRNA signature of Alzheimer disease patients. *Genome Biol*. 2013;14(7):R78. doi:10.1186/gb-2013-14-7-r78
58. Sproviero D, Gagliardi S, Zucca S, et al. Different miRNA profiles in plasma derived small and large extracellular vesicles from patients with neurodegenerative diseases. *Int J Mol Sci*. 2021;22(5):2737. doi:10.3390/ijms22052737

59. Banzhaf-Strathmann J, Benito E, May S, et al. MicroRNA-125b induces tau hyperphosphorylation and cognitive deficits in Alzheimer's disease. *EMBO J*. 2014;33(15):1667-1680. doi:[10.15252/embj.201387576](https://doi.org/10.15252/embj.201387576)
60. Absalon S, Kochanek DM, Raghavan V, Krichevsky AM. MiR-26b, upregulated in Alzheimer's disease, activates cell cycle entry, tau-phosphorylation, and apoptosis in postmitotic neurons. *J Neurosci*. 2013;33(37):14645-14659. doi:[10.1523/JNEUROSCI.1327-13.2013](https://doi.org/10.1523/JNEUROSCI.1327-13.2013)
61. Jia L, Zhu M, Yang J, et al. Prediction of P-tau/Abeta42 in the cerebrospinal fluid with blood microRNAs in Alzheimer's disease. *BMC Med*. 2021;19(1):264. doi:[10.1186/s12916-021-02142-x](https://doi.org/10.1186/s12916-021-02142-x)
62. Wyczechowska D, Harch PG, Mullenix S, et al. Serum microRNAs associated with concussion in football players. *Front Neurol*. 2023;14:1155479. doi:[10.3389/fneur.2023.1155479](https://doi.org/10.3389/fneur.2023.1155479)
63. Lee M, Cho H, Jung SH, et al. Circulating MicroRNA expression levels associated with internet gaming disorder. *Front Psychiatry*. 2018;9:81. doi:[10.3389/fpsy.2018.00081](https://doi.org/10.3389/fpsy.2018.00081)
64. Nuzziello N, Craig F, Simone M, et al. Integrated analysis of microRNA and mRNA expression profiles: An attempt to disentangle the complex interaction network in attention deficit hyperactivity disorder. *Brain Sci*. 2019;9(10):288. doi:[10.3390/brainsci9100288](https://doi.org/10.3390/brainsci9100288)
65. Jakaria M, Belaidi AA, Bush AI, Ayton S. Ferroptosis as a mechanism of neurodegeneration in Alzheimer's disease. *J Neurochem*. 2021;159(5):804-825. doi:[10.1111/jnc.15519](https://doi.org/10.1111/jnc.15519)
66. Roy RG, Mandal PK, Maroon JC. Oxidative stress occurs prior to amyloid abeta plaque formation and tau phosphorylation in Alzheimer's disease: Role of glutathione and metal ions. *ACS Chem Neurosci*. 2023;14(17):2944-2954. doi:[10.1021/acscchemneuro.3c00486](https://doi.org/10.1021/acscchemneuro.3c00486)
67. Milovanovic J, Arsenijevic A, Stojanovic B, et al. Interleukin-17 in chronic inflammatory neurological diseases. *Front Immunol*. 2020;11:947. doi:[10.3389/fimmu.2020.00947](https://doi.org/10.3389/fimmu.2020.00947)

## SUPPORTING INFORMATION

Additional supporting information can be found online in the Supporting Information section at the end of this article.

**How to cite this article:** Krüger DM, Pena-Centeno T, Liu S, et al. The plasma miRNAome in ADNI: Signatures to aid the detection of at-risk individuals. *Alzheimer's Dement*. 2024;20:7479–7494. <https://doi.org/10.1002/alz.14157>